University of Banja Luka I Faculty of Architecture, Civil Engineering and Geodesy
ISSN 2712-057 I E-ISSN 2303-6036 I UDC 72

2022_10(1)

AGG+ Journal for Architecture, Civil Engineering, Geodesy and Related Scientific Fields
АГГ+ часопис за архитектуру, грађевинарство, геодезију и сродне научне области

064-086 **Categorisation** I Original scientific paper
DOI I 10.7251/AGGPLUS/2210064S
UDC I 681.324:519.816(4)
COBISS.RS-ID I **XXXXXXXXXXXXXXXX**
Paper received I 09/10/2022
Paper accepted I 20/10/2022

Jakob Šušteršič
IRMA Institute for Research in Materials and Applications, Slovenia, jakob.sustersic@irma.si

Rok Ercegovič
IRMA Institute for Research in Materials and Applications, Slovenia, rok.ercegovic@guest.arnes.si

David Polanec
IRMA Institute for Research in Materials and Applications, Slovenia, david.polanec@irma.si

Bojana Grujić
University of Banja Luka, Faculty of Architecture, Civil Engineering and Geodesy, Bosnia and Herzegovina, bojana.grujic@aggf.unibl.org

EVALUATION OF THE RESISTANCE TO CRACK PROPAGATION OF HIGH-PERFORMANCE CONCRETES BY THE WEDGE SPLITTING TEST METHOD

Original scientific paper
DOI 10.7251/AGGPLUS/2210064S
UDC 681.324:519.816(4)
COBISS.RS-ID XXXXXXXXXXXXXXXXX
Paper received I 09/10/2022
Paper accepted I 20/10/2022

* corresponding author

This paper is an extended version of the paper previously published in the Proceedings of STEPGRAD2022 International Conference.

Jakob Šušteršič
IRMA Institute for Research in Materials and Applications, Slovenia, jakob.sustersic@irma.si

Rok Ercegovič
IRMA Institute for Research in Materials and Applications, Slovenia, rok.ercegovic@guest.arnes.si

David Polanec
IRMA Institute for Research in Materials and Applications, Slovenia, david.polanec@irma.si

Bojana Grujić *
University of Banja Luka, Faculty of Architecture, Civil Engineering and Geodesy, Bosnia and Herzegovina, bojana.grujic@agqf.unibl.org

EVALUATION OF THE RESISTANCE TO CRACK PROPAGATION OF HIGH-PERFORMANCE CONCRETES BY THE WEDGE SPLITTING TEST METHOD

ABSTRACT

This paper describes the key elements of the results of investigations on the resistance to crack propagation carried out as part of a large-scale project to develop high-performance concretes (HPCs) for the secondary lining of a low and intermediate-level waste disposal shaft. Four HPCs were investigated, in which the quantity of the binder component and the proportions of the two cements and the silica fume in it were varied. We have also added steel fibers to one HPC. The wedgesplitting test method was used to determine the resistance to crack propagation. The results obtained show that all the HPC investigated achieve good resistance to crack propagation. The addition of steel fibers further improves this resistance.

***Keywords**: resistance to crack propagation, high-performance concrete, wedge splitting test*

1. INTRODUCTION

High-performance concrete (HPC) differs from normal concrete in at least one individual property (compressive strength, permeability, workability or other) and in structure, composition, and production [1]. Research during the 1970s, highly effective plasticizers or superplasticizers for concrete introduced the possibility of significantly reducing the value of the w/c ratio and achieving, regardless of the moderate content of cement, a high degree of workability. The low value of the w/c ratio, with good compaction, has a significant contribution to high strengths. Strength was an important parameter in distinguishing HPC from normal concrete.

In the 1950s, the compressive strength of concrete was considered to be 35 MPa high strength [2]. In the 1960s, concretes with compressive strengths of up to 40 and 50 MPa were used. The European Standard for Concrete EN 206:2013 defines in clause 4.3.1 "Compressive strength classes" in Table 12 "Compressive strength classes for normal and heavy concrete", ending at compressive strength class C 100/115, and Table 13 "Compressive strength classes for lightweight concrete", ending at compressive strength class LC 80/88. The tables are identical to those in the previous edition of EN 206-1:2003. Neither of the two editions of the concrete standard gives any rules for high-strength concretes. It should be noted that the old edition of EN 206-1:2003, among the definitions in Chapter 3 "Definitions, symbols and abbreviations", clause 3.1.10 defined that high-strength concretes are normal concretes of strength class C 55/67 and above and lightweight concretes of strength class LC 50/55 and above. This definition is not in the new edition of EN 206:2013.

Strengths up to 150 MPa were a sensation [3]. Using special technologies and materials in laboratories and experimental productions, compressive strengths of 230 MPa and 460 MPa [2] and up to 800 MPa and more have been achieved [4], so-called concretes with reactive powder RPC (Reactive Powder Concrete) [5, 6]. The first applications of high-strength concretes were recorded during the construction of highly loaded columns of tall buildings (skyscrapers) [7, 8].

Over time, it became known that high-strength concrete improves other properties, such as abrasion resistance, capillary absorption, gas permeability and water permeability, diffusion resistance, resistance to freezing-thawing in the presence of de-icing salts, etc. Due to these improvements, the term high-performance concrete (HPC) [9] was introduced. The HPC concept has been extended to fresh concrete so that self-consolidating concrete (SCC) [10] is also considered HPC.

High-strength concrete is achieved by maximizing the densification of the structure of the hardened cement paste and the densification of the transition zone of the interfaces between the hardened cement paste and the aggregate grains. First, we need to achieve a good "packing" of the aggregate grains [11] or a compacted aggregate structure that is "glued" with cement paste.

Mineral admixtures as well as polymers are very often used to achieve the densest structure of the hardened cement paste and the most dense transition zone. In this case, we are not talking about a water-cement (w/c) ratio but a water-binder (w/b) ratio. Higher concrete strength is achieved by increasing the quantity of mineral admixtures and decreasing the w/b ratio. But often, increasing the quantity of mineral admixtures increases the need for water. In such a case, when the critical quantity of a given mineral admixture is exceeded,

the strength of concrete is reduced because the w/b ratio is increased. Therefore, when mineral admixtures are used, highly effective plasticizers are added to concrete to evenly distribute the fine particles of the mineral admixture and reduce the amount of water, thus increasing the strength of the concrete. In any case, the amount of mineral admixtures is also limited for other reasons, which were discussed in much more detail at the 22nd Slovenian Colloquium on Concretes: Use of mineral admixtures in cement and/or concrete [12].

Typically, the w/b ratio values of high-strength concretes are between 0,25 and 0,40. At such low w/b ratios, not all the binding components (cement and mineral admixtures) hydrate. The lower the w/b ratio, the more non-hydrated particles there are, the density increases and the strength of the concrete increases [13]. Non-hydrated cement and mineral additive particles act as mineral fillers.

Hardened cement paste binds the aggregate grains together. Physical interactions are mainly dominant, and chemical bonding is rare. On the surfaces of the aggregate grains, crystals grow from the highly saturated solution, i.e., calcium-hydroxyl lamellae. Investigations show that conventional cement paste produces a porous layer with a crystalline orientation on the surfaces of the aggregate grains, with a thickness of about 40 µm. This layer has a lower hardness and strength than hardened cement paste. Investigations show that the thickness of the transition zone is difficult to influence by varying the w/c ratio, like the average aggregate grain spacing in concrete, which is approximately 75 to 100 µm [14]. As a consequence, the mechanical properties of concrete are highly dependent on the transition zone. SEM photos [15] show that there is a dense, irregular zone with a thickness of 1 µm on the surface of the aggregate grains. This zone is followed by a porous transition zone about 10 µm thick.

It can be observed that the porosity of the transition zone decreases as the concrete hardens, while that of the compact cement paste remains relatively constant. However, the transition zone can be significantly densified by adding mineral admixtures. Silica fume is the most effective because the small particles increase the volume around the cement particle and hydrate significantly faster than fly ash or slag due to their large specific surface area. In addition, CH is transformed into CSH, reducing the amount of CH crystals at the interface between the hardened cement paste and the aggregate grains.

The reduction of porosity, or densification of the transition zone by mineral admixtures, greatly reduces the possibility of cracks forming during the application of external loads at the interface between the hardened cement paste and the aggregate grains. This increases the strength of the concrete.

The influence of the good bond between the hardened cement paste and the aggregate grains, or the densified transition zone due to the addition of silica fume, can be seen in the photographs in Figure 1, which show the surfaces of the concrete test specimens (cubes) after the wedge splitting test [16].

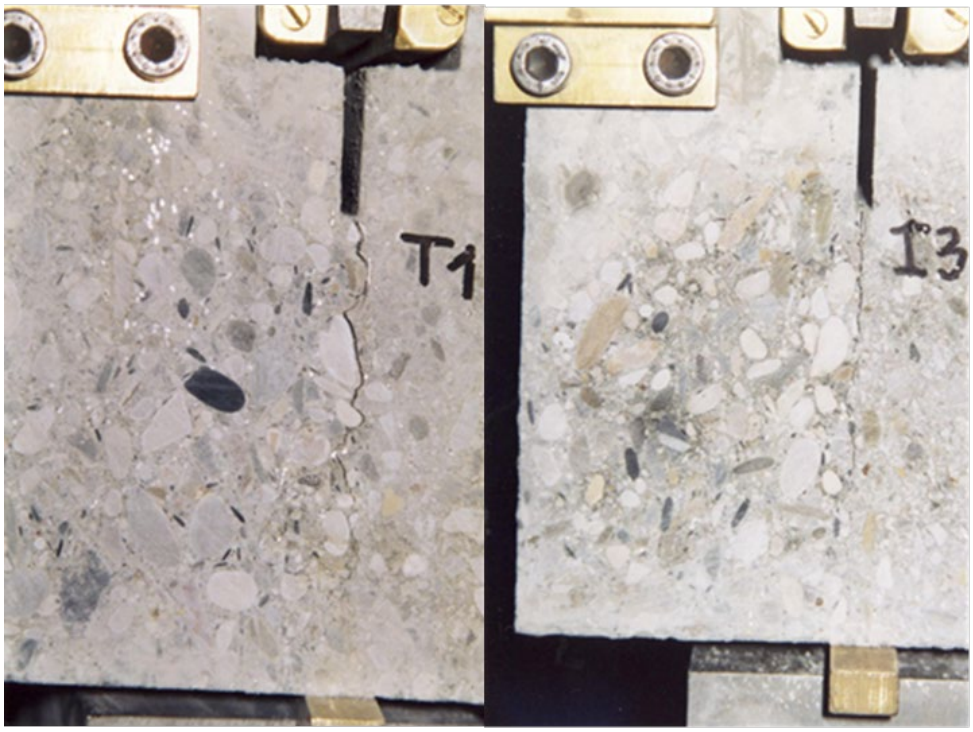

***Figure 1**. Surface photographs of concrete cubes after wedge splitting test: (a) concrete without mineral admixture, (b) concrete with added silica fume [16].*

The addition of silica fume (7,5 % w/w of cement) to the concrete - right picture (b) in Figure 1 - has densified the transition zones, and they no longer represent the weak or porous regions in the concrete that would be the cause of the crack initiation and propagation. Also, adding silica fume makes the cement paste denser, which means there are far fewer weak regions in the concrete where cracks would start to form. As the external load continues to be applied, these cracks join to form a single dominant crack, which ultimately leads to the concrete test specimen collapsing.

In general, the propagation of cracks can be said to depend on the magnitude and duration of stresses that caused their formation and the external loads. Concrete resists this expansion by bridging the cracks with aggregate grains and, additionally if present, with fibers or polymer. We are talking about the resistance of concrete to crack propagation or the ability of concrete to absorb as much energy as possible up to a certain (chosen) crack width.

2. METHOD FOR DETERMINING THE RESISTANCE TO CRACK PROPAGATION

The resistance to crack propagation of concrete is determined by the following equation:

$$RCP = \frac{f_{ct}}{f_{cw}} \tag{1}$$

where:

RCP - resistance to crack propagation,

f_{ct} - ultimate splitting tensile strength (MPa),

f_{CW} - equivalent splitting tensile strength up to the selected crack width (MPa).

In practice, the equivalent splitting tensile strength up to a crack width of 0.2 mm ($f_{0,2}$) is most used to calculate the resistance of concrete to crack propagation, and equation (1) takes the following form [21]:

$$RCP = \frac{f_{ct}}{f_{0,2}} \quad (2)$$

where:

RCP - resistance to crack propagation,

f_{ct} - ultimate splitting tensile strength (MPa),

$f_{0,2}$ - equivalent splitting tensile strength up to the crack width of 0,2 mm (MPa).

From the load - CMOD (Crack Mouth Opening Displacement) diagrams, the ultimate splitting tensile strength (f_{ct}) and the equivalent splitting tensile strengths up to crack widths CW = 0,1, 0,2, 0,3 and 0,4 mm (f_{CW}) are determined or calculated. The load - CMOD diagram was obtained during the wedge splitting test of concrete. The wedge splitting test (WST) method, which produces a load - CMOD diagram, is one of many test methods developed to determine the behavior of cement-based composites in the cracked state. The WST method we use was developed by Tschegg and Linsbauer [17-20] and is briefly described below.

A test specimen (cube) with a rectangular groove and a notch at the bottom of the groove is placed on a flat linear support in a compression testing machine (Figure 2). The two transfer pieces inserted in the groove cause the test specimen to split by pushing the wedge in.

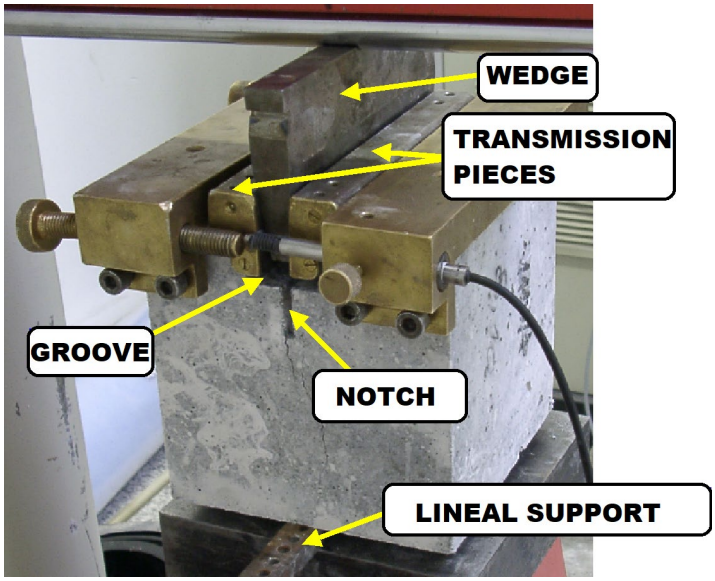

***Figure 2**: Individual components of the wedge splitting test device*

The force F (Figure 3) caused by the compression testing machine is transmitted by the wedge to the test specimen by dividing it into two components. The larger horizontal component F_H splits the test specimen.

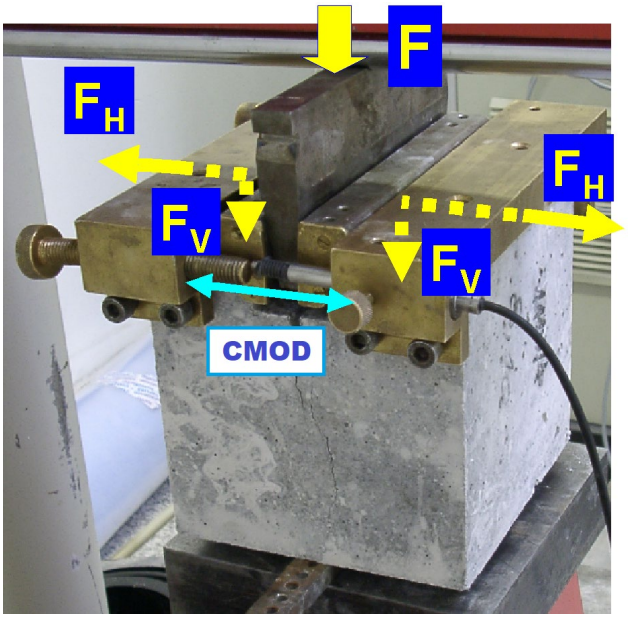

***Figure 3**: Principle of the wedge splitting test method*

The smaller vertical component F_V helps to control the direction of crack propagation in the plane connecting the support and the notch. As the wedge angle is small, the F_V component does not affect the test results. The deformation is determined by measuring the Crack Mouth Opening Displacement (CMOD) in the line of action of the F_H component during the splitting of the test specimen.

During the application of a load to the test specimen, small individual cracks within the concrete begin to appear at a given load. These cracks join to form a continuous crack that can be seen on the surface of the test specimen. At this point in the load - CMOD diagram, the slope of the diagram increases sharply. The load and CMOD at this point are referred to as the load at the first crack F_{fc} and the Crack Mouth Opening Displacement at the first crack $CMOD_{fc}$, respectively.

There are difficulties relating to the precise determination of the location of the first crack (FC). ASTM C 1018 defines the first crack as the point on the load – CMOD diagram at which the curve form first becomes non-linear. Determination of the point of FC has been proposed [22, 23] as the point at which the slope of the curve departs from linearity by more than 5 % and lasts for an interval of more than 0,01 mm.

At our Institute (IRMA), a computer program, which works in graphical form, has been developed for automatically drawing load - CMOD curves, calculation of parameters for evaluation of concrete behavior, and determination of the point of FC [24].

At the moment when the point FC is reached, the crack width begins to propagate with further loading. From the point FC, the fracture zone of the concrete begins to form. In the

fracture zone, all further fracture processes proceed until the final separation of the test specimen.

3. EXPERIMENTAL BASIS

3.1. SHORT INTRODUCTION TO THE PROJECT

The project briefly reviewed here is entitled “Study on the production, placeability and characteristics of final concrete mixtures for the construction of secondary reinforced concrete lining of the silo of the LILW repository” [25]. The project was carried out at the Institute for Research in Materials and Applications (IRMA), in the laboratory and the test field. The implementation was carried out by the laboratories of the Slovenian National Building and Civil Engineering Institute (ZAG), the Faculty of Civil and Geodetic Engineering of the University of Ljubljana, the Geological Survey of Slovenia, Salonit Anhovo and the Faculty of Civil Engineering of the University of Zagreb. HSE Invest and IBE, the designer of the LILW repository, worked together on specific areas of expertise. During the project implementation, we worked closely with the project sponsor, the Agency for Radioactive Waste (ARAO).

The project was implemented in three phases. The results and findings of each phase served as a basis for the continuation of the project in the next phase. So, in the first phase, we selected the basic materials and carried out preliminary tests on the concretes. Based on the results obtained, four optimum concrete mix proportions were identified and tested in the laboratories as part of the second phase. We investigated the properties of fresh and hardened concretes relevant for achieving extremely high concrete durability and service life of the secondary lining and, indirectly, of the entire LILW silo. These results were confirmed by measurements and investigations in the test field during the first part of the third phase of the project. The measurements and investigations in the test field also provided new results and findings, which were used to develop the basic technological parameters for the construction of the secondary reinforced concrete lining of the silo of the LILW repository. These were prepared as part of the second part of the third phase of the project.

3.2. SELECTION OF BASIC MATERIALS AND IDENTIFICATION OF CONCRETE MIX PROPORTIONS

3.2.1. Binder

The selection of the binder was based on the key required characteristics of the concrete:

- high compressive strength,
- low development of hydration heat,
- low permeability,
- sulphate resistance,
- extremely high durability of the concrete and the service life of the completed structure.

There is no such binder on the market that meets the above requirements. Therefore, we selected a binder component consisting of two types of cement (CEM I 42,5 N SRO and CEM III/B 32,5 N - LH/SR) and Silica Fume (SF).

3.2.2. Aggregate

The gravels from the Lower Sava separations, which are located close to the LILW disposal site, are not an option due to the presence of coal grains. Dolomite or limestone crushed aggregate have been proposed as possible aggregate types. Based on a literature review of the findings of several studies of concretes with dolomite and limestone aggregate, we chose limestone aggregate mainly because of the potential for an alkali-dolomite reaction in concrete with dolomite aggregate at high concrete ages. The concretes investigated in this project were prepared using crushed quarry aggregate of carbonate origin with more than 96% limestone or calcium carbonate.

3.2.3. Chemical admixtures

The selection of the chemical admixtures was carried out in the framework of preliminary tests of the concretes regarding the workability and air content of the fresh concrete.

3.2.4. Steel fibers

To obtain the optimum concrete mix proportion according to the given criteria, the mix proportions were modified by adding steel fibers. To minimize the effect of the fibers on the workability of the fresh concrete and to maximize the uniform distribution of fibers in the fresh concrete mass, short (16 mm long) and thin (0,4 mm thick) steel fibers with anchors at the ends were selected to allow good anchorage in the hardened concrete matrix.

3.2.5. Concrete mix-proportions

Based on the results of the preliminary investigations, four mix-proportions of concrete or High-Performance Concrete (HPC), respectively (Table 1) were determined, which were investigated in the laboratories during the second phase of the project, placed in the test field and investigated during the first part of the third phase.

Table 1. *Mix-proportions of High-Performance Concrete (HPC)*

Parameter	Unit	Designations of HPC			
		PP-1	PP-1-JV	PP-2	PP-3
Binder (CEM I + CEM III + SF)	(kg/m^3)	405	405	405	425
CEM I / CEM III	-	0.43	0.43	1.00	1.00
Hyper-plasticizer	(% m/m)	0.47	0.47	0.47	0.78
Antifoaming admixture	(% m/m)	1.00	1.00	1.00	1.00
$(w/b)_{eff.design}$	-	0.38	0.38	0.38	0.38
Steel fibers	(% v/v)	-	0.77	-	-
D_{max} of limestone aggregate	(mm)	32	32	32	32

3.3. OVERVIEW OF THE RESULTS OF SOME PROPERTIES OF HARDENED HPC

In this section, we would like to provide additional information on only some of the properties of all four HPCs that sufficiently represent their characteristics.

3.3.1. Compressive strength

The compressive strength according to SIST EN 12390-3:2009 of the hardened HPC was tested at ages 1, 2, 3, 7, 28, 56 and 154 days. Figure 4 shows the average compressive strength results as a function of the age of the HPC.

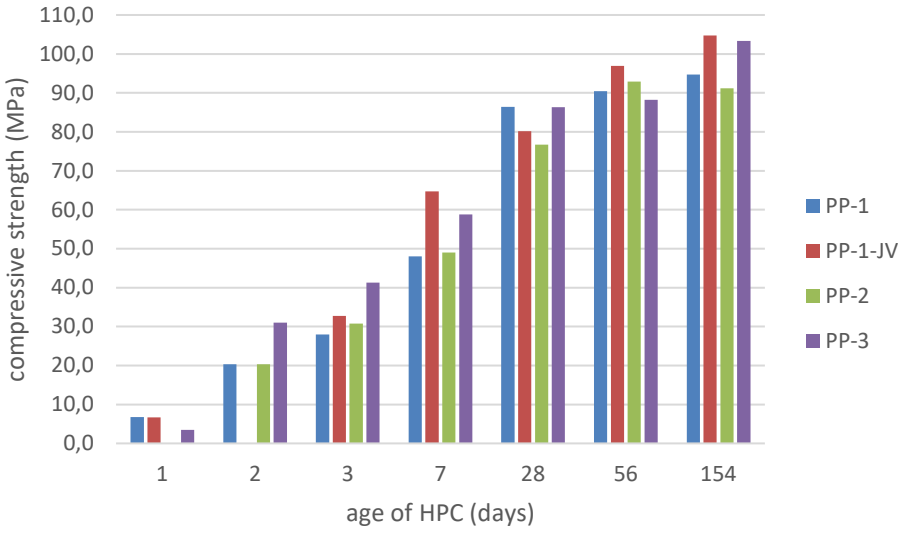

***Figure 4**. Average compressive strength values as a function of HPC age*

The project requires a compressive strength class of C60/75 at 90 days. As we have not been able to determine the compressive strength of the HPC at 90 days of age, we give an estimate of the compressive strength class achieved at 56 and 154 days of age. The assessment (according to SIST EN 206:2013, Appendix A) shows that all HPCs meet the criteria of the required compressive strength class C60/75 at 56 and 154 days of age, which means that they also meet this criterion at 90 days. PP-1-JV and PP-3 also meet the criteria for the higher class C70/85 at 154 days of age.

3.3.2. Static modulus of elasticity

Static modulus of elasticity tests were carried out according to DIN 1048-5:1991 at HPC ages of 7, 28, 56 and 90 days. Figure 5 shows the average results of the static modulus of elasticity as a function of the age of the HPC.

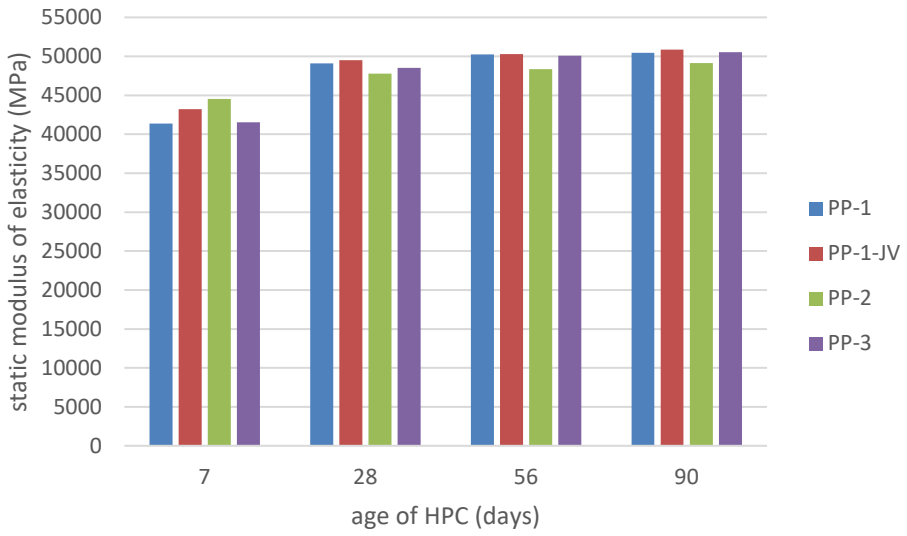

***Figure 5**. Average static modulus of elasticity as a function of HPC age*

The average test results of all HPC at 28 days of age meet the criterion ($E_{stat,28} \leq 50000$ MPa). At ages 56 and 90 days, the E_{stat} values increase only slightly and are slightly greater than 50000 MPa for PP-1, PP-1-JV and PP-3. For PP-2, the E_{stat} is < 50000 MPa even at age 90 days.

3.3.3. Resistance to water penetration

Water penetration tests according to SIST EN 12390-8.2009 were carried out at HPC ages of 7, 28, 56 and 90 days. Figure 6 shows the average results of the water penetration tests as a function of the age of the HPC.

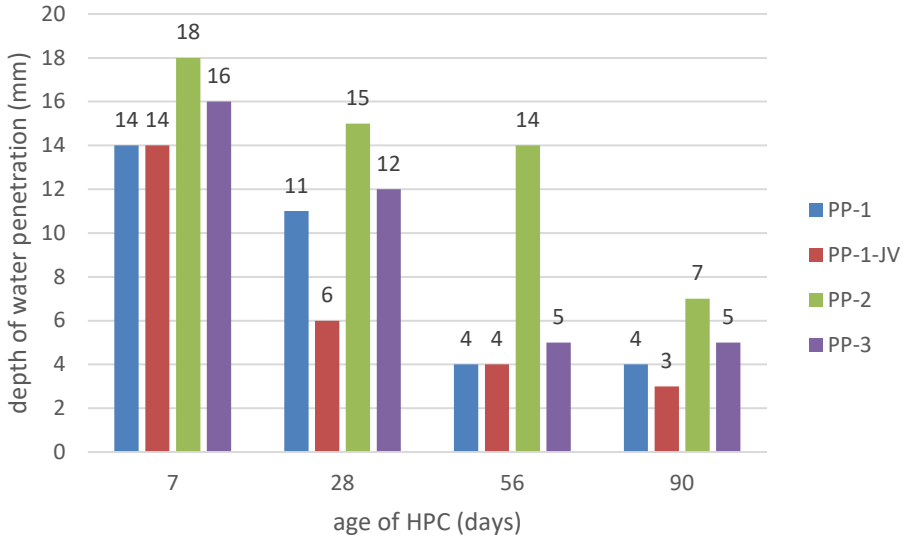

***Figure 6.** Average depth of water penetration as a function of HPC age.*

The following project requirements are given:

- maximum average allowed depth of water penetration: $e_{aver,allow}$ = 10 mm,
- maximum individual allowed result: $e_{max,allow}$ = 15 mm.

As HPC increase in age, their resistance to water penetration increases. PP-1-JV already meets the required criterion at 28 days of age, PP-1 and PP-3 at 56 days of age and PP-2 only at 90 days of age.

3.3.4. Internal freeze/thaw resistance

The internal freeze/thaw resistance test is performed at HPC ages 56 and 90 days, according to SIST 1026:2016, Appendix ND. In Table 2, we report the average and minimum relative dynamic modulus of elasticity after n freeze/thaw cycles of all four HPC mixtures that we started testing at ages 56 and 90 days.

Table 2. *Average and minimum relative dynamic modulus of elasticity after n freeze/thaw cycles*

HPC	Age of HPC at the start of the test (days)	Number of cycles n	Relative dynamic modulus of elasticity	
			Average (%)	Minimum (%)
PP-1	56	375	95.8	92.1
	90	325	97.4	97.0
PP-1-JV	56	375	98.1	97.7
	90	300	98.8	98.5
PP-2	56	375	96.8	92.1
	90	300	97.4	95.5
PP-3	56	350	99.9	98.9
	90	275	99.0	98.4

Although the required criterion for internal freeze/thaw resistance is up to 200 cycles, all HPCs were tested up to n cycles (see Table 2). Even after n cycles, all HPCs met the criterion: average relative dynamic modulus of elasticity > 80% and minimum relative dynamic modulus of elasticity > 75%. Based on these results, it can also be roughly estimated that all four HPCs have a quality structure that can assure the long service life of the LILW repository.

3.3.5. Resistance to chloride diffusion

According to the method given in NT BUILD 492:1999, the resistance to chloride diffusion test was carried out at HPC ages of 56 and 90 days. Table 3 gives the results of the average chloride diffusion coefficients.

Table 3*. Average coefficients of chloride diffusion*

HPC	$D_{nssm,} \times 10^{-12}$ m²/s	$D_{nssm,} \times 10^{-12}$ m²/s
	Age of HPC 56 days	Age of HPC 90 days
PP-1	0,77 ± 0,28	0,55 ± 0,05
PP-1-JV	1,48 ± 0,23	1,01 ± 0,18
PP-2	1,16 ± 0,13	0,71 ± 0,05
PP-3	0,86 ± 0,09	0,68 ± 0,10

All HPCs meet the criterion for the coefficient of chloride diffusion $D_{nssm} \leq 9{,}0\ 10^{-12}\ m^2/s$.

4. RESULTS OF RESISTANCE TO CRACK PROPAGATION TESTS AND DISCUSSION

All four HPCs were tested by the WST method described in section 2 at 3, 7, 28, 56 and 90 days of age. For each test specimen, we first determined the load – CMOD diagram. From the shape of the diagram, we can already assess the behavior of the test specimen during the application of the splitting load. As an example, we give in Figure 7 the typical load - CMOD diagrams determined for PP-1, PP-1-JV, PP-2 and PP-3 at their age of 90 days.

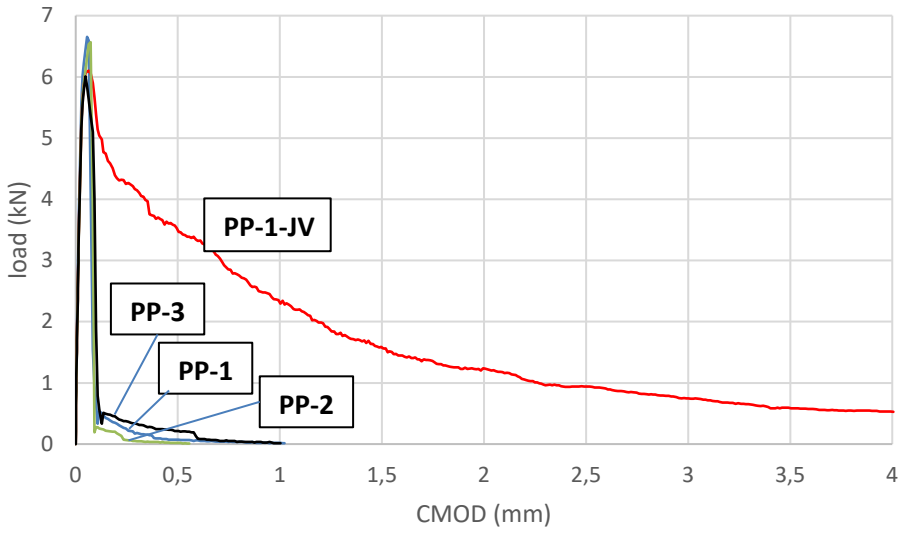

***Figure 7**. Typical load - CMOD diagrams of PP-1, PP-1-JV, PP-2 and PP-3 at 90 days of age.*

We can immediately estimate that much more energy was absorbed during the PP-1-JV test compared to the other HPCs. This is understandable, of course, because PP-1-JV contains steel fibers, while the other HPCs are without fibers. A similar assessment can be made based on a visual inspection of the test specimens after the WST (Figure 8a, b, c). The cracks on test specimens PP-1 (a) and PP-3 (b) run more or less vertically to the lower edge - the cubes have split into two parts. In contrast, the cracks on the PP-1-JV (c) specimens are very branched and do not reach the lower edge of the cube. The cube does not break because the fibers bridge the crack and offer great resistance to crack propagation.

(a)

(b)

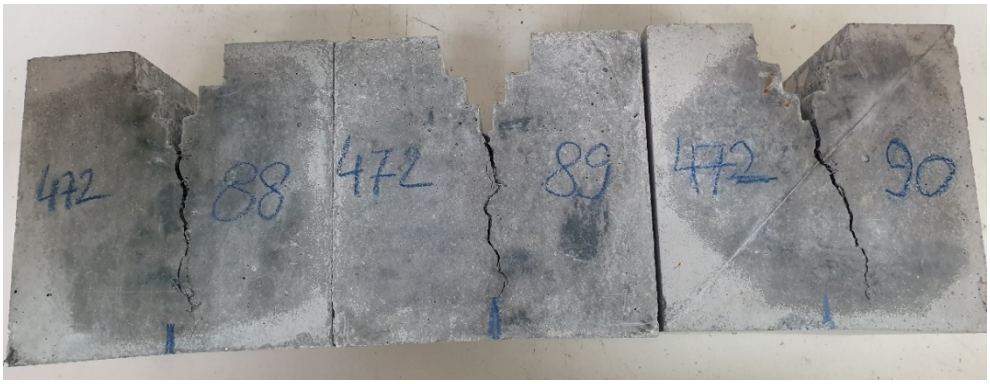

(c)

Figure 8. *Crack shape and course after completion of WST on PP-1 (a), PP-3 (b) and PP-1-JV (c) specimens at 90 days of age.*

The estimate described above is rough and relative. However, if we want to have a more accurate and measurably comparable estimate, we need to determine and calculate the parameters from the load - CMOD diagrams, as we have already described in section 2.

These parameters are:

- f_{ct} - ultimate splitting tensile strength,
- f_{fc} - splitting tensile strength at the first crack,

- f_{CW} - equivalent splitting tensile strength up to the crack width CW = 0,1, 0,2, 0,3 and 0,4 mm,
- RCP (Resistance to Crack Propagation) = $f_{0,2}/f_{ct}$.

For all HPCs, we summarize the resulting parameters in Table 4 for PP-1, Table 5 for PP-1-JV, Table 6 for PP-2 and Table 7 for PP-3. For each table, the corresponding equivalent splitting tensile strengths f_{CW} versus crack width CW are given in the graphical form.

Table 4. *Results of the wedge splitting test for PP-1.*

designation of the test specimen	age of PP-1	ultimate splitting tesnile strength - f_{ct}	splitting tensile strength at first crack - f_{fc}	equivalent splitting tensile strength up to the crack width (mm)				resistance to crack propagation RCP=$f_{0,2}/f_{ct}$
				0,1	0,2	0,3	0,4	
				$f_{0,1}$	$f_{0,2}$	$f_{0,3}$	$f_{0,4}$	
	(days)	(MPa)	(MPa)	(MPa)	(MPa)	(MPa)	(MPa)	-
PP-1/19	6	3,47	3,33	2,72	2,03	1,60	1,36	0,59
PP-1/20		3,78	3,54	3,28	2,51	2,01	1,67	0,66
PP-1/21		3,39	3,09	2,81	2,36	1,93	1,61	0,70
average		**3,55**	**3,32**	**2,94**	**2,30**	**1,85**	**1,55**	**0,65**
PP-1/22	8	4,22	3,94	3,64	2,69	2,00	1,60	0,64
PP-1/23		4,08	3,61	3,28	2,58	2,00	1,62	0,63
PP-1/24		4,38	4,15	3,46	2,88	2,36	1,97	0,66
average		**4,23**	**3,90**	**3,46**	**2,72**	**2,12**	**1,73**	**0,64**
PP-1/25	28	4,90	4,78	4,07	3,21	2,40	1,90	0,66
PP-1/26		4,94	4,78	4,36	3,40	2,60	2,11	0,69
PP-1/27		4,64	3,53	3,55	2,84	2,21	1,78	0,61
average		**4,83**	**4,36**	**3,99**	**3,15**	**2,40**	**1,93**	**0,65**
PP-1/28	56	5,71	5,32	4,68	3,92	3,03	2,34	0,69
PP-1/29		5,84	5,63	4,36	3,61	2,65	2,08	0,62
PP-1/30		5,45	5,16	4,65	3,81	2,85	2,25	0,70
average		**5,67**	**5,37**	**4,56**	**3,78**	**2,84**	**2,22**	**0,67**
PP-1/88	90	6,91	6,23	5,27	4,22	3,09	2,41	0,61
PP-1/89		6,35	5,74	4,36	3,93	2,85	2,24	0,62
PP-1/90		5,72	5,29	4,53	3,67	2,69	2,11	0,64
average		**6,33**	**5,75**	**4,72**	**3,94**	**2,88**	**2,25**	**0,62**

After the first crack, and as the crack width increases, the equivalent strengths decrease (Figure 8). This is known as softening. The increase in equivalent strengths at a given crack width is more moderate compared to the increase in f_{ct} (third column in table 4) up to the age of PP-1 56 days. Thereafter, the equivalent strengths increase only slightly up to 90 days of age.

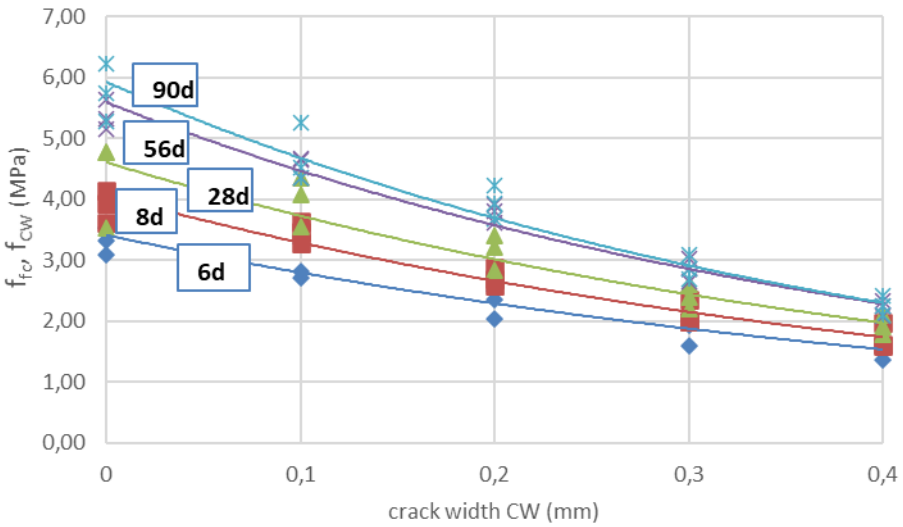

Figure 8. *Equivalent splitting tensile strengths f_{cw} and splitting tensile strength at first crack f_{fc} of PP-1 as a function of crack width.*

In the light of the above observation, a moderate increase in resistance to crack propagation RCP up to the age of PP-1 56 days is understandable, and then it decreases at the age of 90 days (last column in Table 4). RCP > 0.60 at all ages PP-1.

Table 5. *Results of the wedge splitting test for PP-1-JV.*

designation of the test specimen	age of PP-1-JV	ultimate splitting tesnile strength - f_{ct}	splitting tensile strength at first crack - f_{fc}	equivalent splitting tensile strength up to the crack width (mm)				resistance to crack propagation RCP=$f_{0,2}/f_{ct}$
				0,1	0,2	0,3	0,4	
				$f_{0,1}$	$f_{0,2}$	$f_{0,3}$	$f_{0,4}$	
	(days)	(MPa)	(MPa)	(MPa)	(MPa)	(MPa)	(MPa)	-
PP-1-JV/1	3	3,50	3,01	3,15	2,87	2,72	2,59	0,82
PP-1-JV/2		3,99	3,49	3,55	3,39	3,20	3,15	0,85
PP-1-JV/2		3,63	3,27	3,05	2,72	2,50	2,43	0,75
average		**3,71**	**3,26**	**3,25**	**2,99**	**2,81**	**2,72**	**0,81**
PP-1-JV/2	8	6,07	5,81	4,79	4,54	4,13	3,97	0,75
PP-1-JV/2		5,54	4,49	4,83	4,37	3,83	3,60	0,79
PP-1-JV/2		4,86	3,72	4,07	3,87	3,51	3,37	0,80
average		**5,49**	**4,67**	**4,56**	**4,26**	**3,82**	**3,65**	**0,78**
PP-1-JV/2	28	5,36	4,34	4,31	4,70	4,73	4,82	0,88
PP-1-JV/2		4,79	4,14	4,01	4,30	4,32	4,29	0,90
PP-1-JV/2		4,82	4,25	4,18	4,42	4,28	4,25	0,92
average		**4,99**	**4,24**	**4,17**	**4,47**	**4,44**	**4,45**	**0,90**
PP-1-JV/2	56	5,79	4,36	5,05	4,63	4,16	3,97	0,80
PP-1-JV/2		6,01	4,42	4,93	4,54	4,06	3,86	0,76
PP-1-JV/3		6,24	5,00	4,96	4,68	4,38	4,28	0,75
average		**6,01**	**4,59**	**4,98**	**4,62**	**4,20**	**4,04**	**0,77**
PP-1-JV/8	90	5,41	4,13	4,62	4,53	4,46	4,41	0,84
PP-1-JV/8		5,95	5,11	5,00	4,67	4,60	4,32	0,78
PP-1-JV/9		6,10	5,22	4,94	4,83	2,69	2,11	0,79
average		**5,82**	**4,82**	**4,85**	**4,68**	**3,92**	**3,61**	**0,80**

The ultimate splitting tensile strength f_{ct} increases unevenly with the age of PP-1-JV (third column in Table 5). After the first crack, and as the crack width increases, the equivalent strengths decrease moderately (Figure 9). Softening is moderate. For a given crack width, the equivalent strengths increase significantly from PP-1-JV age of 3 days to 8 days. Thereafter, the equivalent strengths increase relatively less and rather unevenly up to the age of 90 days.

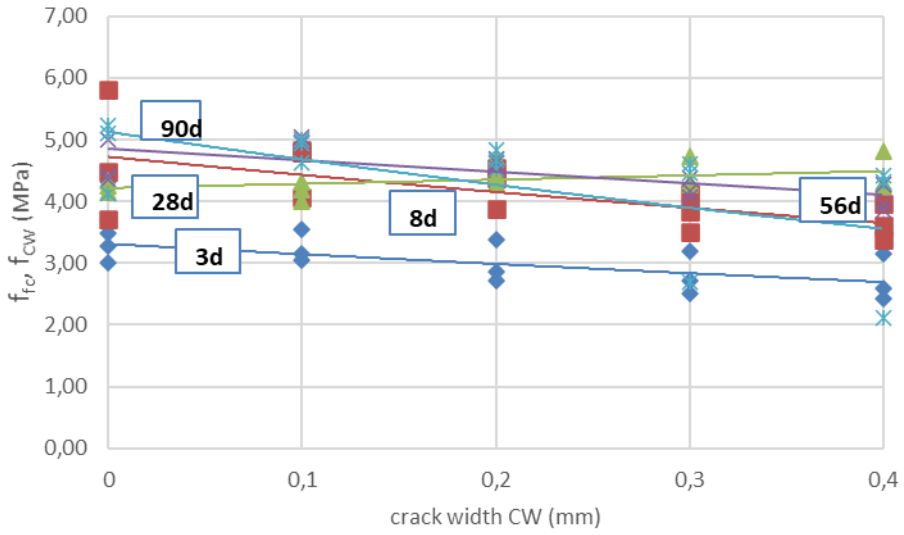

Figure 9. *Equivalent splitting tensile strengths f_{cw} and splitting tensile strength at first crack f_{fc} of PP-1-JV as a function of crack width.*

The RCP also varies in a similar way at different ages of PP-1-JV; average RCP values from age 3 to 90 days are around 0,80 (last column in Table 5). Regardless of the heterogeneity, all individual RCP results ≥ 0,75, which means that PP-1-JV shows good resistance to crack propagation.

Table 6. *Results of the wedge splitting test for PP-2.*

designation of the test specimen	age of PP-2	ultimate splitting tesnile strength - f_{ct}	splitting tensile strength at first crack - f_{fc}	equivalent splitting tensile strength up to the crack width (mm)				resistance to crack propagation RCP=$f_{0,2}/f_{ct}$
				0,1	0,2	0,3	0,4	
				$f_{0,1}$	$f_{0,2}$	$f_{0,3}$	$f_{0,4}$	
	(days)	(MPa)	(MPa)	(MPa)	(MPa)	(MPa)	(MPa)	-
PP-2/19	4	3,42	2,41	2,58	2,20	1,86	1,59	0,64
PP-2/20		3,55	2,67	2,94	2,48	2,10	1,80	0,70
PP-2/21		3,20	2,18	2,78	2,19	1,92	1,70	0,68
average		**3,39**	**2,42**	**2,77**	**2,29**	**1,96**	**1,70**	**0,68**
PP-2/22	7	4,89	3,78	3,99	2,94	2,30	1,88	0,60
PP-2/23		3,81	2,63	3,07	2,25	1,75	1,44	0,59
PP-2/24		3,90	3,06	3,44	2,72	2,18	1,78	0,70
average		**4,20**	**3,16**	**3,50**	**2,64**	**2,08**	**1,70**	**0,63**
PP-2/25	27	5,65	5,11	4,61	3,54	2,75	2,25	0,63
PP-2/26		4,74	3,45	4,03	3,41	2,51	1,99	0,72
PP-2/27		4,96	4,82	4,18	3,18	2,34	1,87	0,64
average		**5,12**	**4,46**	**4,27**	**3,38**	**2,53**	**2,04**	**0,66**
PP-2/28	56	5,43	4,20	4,36	3,75	2,87	2,30	0,69
PP-2/29		6,04	4,40	4,81	3,98	2,97	2,39	0,66
PP-2/30		5,97	5,94	4,56	3,66	3,09	2,62	0,61
average		**5,81**	**4,85**	**4,58**	**3,80**	**2,98**	**2,44**	**0,65**
PP-2/88	90	6,26	5,61	4,81	3,55	2,57	1,89	0,57
PP-2/89		5,85	4,59	4,76	3,79	2,81	2,23	0,65
PP-2/90		6,45	4,92	5,35	4,39	3,29	2,59	0,68
average		**6,19**	**5,04**	**4,97**	**3,91**	**2,89**	**2,24**	**0,63**

The ultimate splitting tensile strength f_{ct} increases uniformly with the age of PP-2 (third column in Table 6). After the first crack, the equivalent strengths decrease as the crack width increases (Figure 10). Softening occurs. The equivalent strengths at a given crack width increase more rapidly from 4 to 27 days of age than from 27 to 90 days.

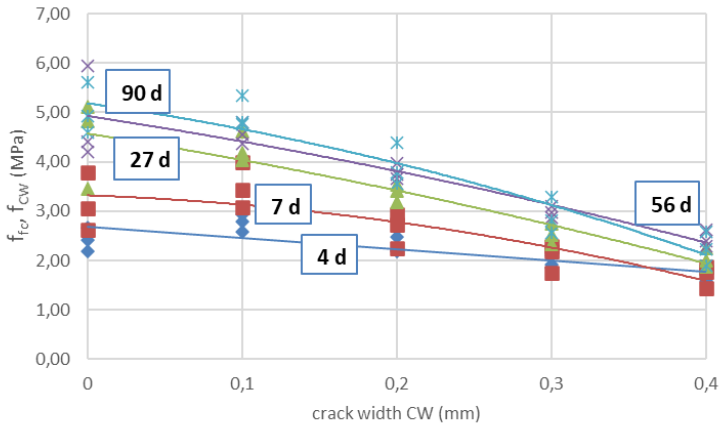

Figure 10*. Equivalent splitting tensile strengths f_{CW} and splitting tensile strength at the first crack f_{fc} of PP-2 as a function of crack width.*

The RCP decreases moderately from age 27 to 90 days (last column in Table 6). All average values are > 0,60

Table 7. *Results of the wedge splitting test for PP-3.*

designation of the test specimen	age of PP-3	ultimate splitting tesnile strength - f_{ct}	splitting tensile strength at first crack - f_{fc}	equivalent splitting tensile strength up to the crack width (mm)				resistance to crack propagation RCP=$f_{0,2}/f_{ct}$
				0,1	0,2	0,3	0,4	
				$f_{0,1}$	$f_{0,2}$	$f_{0,3}$	$f_{0,4}$	
	(days)	(MPa)	(MPa)	(MPa)	(MPa)	(MPa)	(MPa)	-
PP-3/19	3	3,20	2,78	2,73	2,03	1,64	1,37	0,63
PP-3/20		3,27	2,81	2,68	2,28	1,82	1,50	0,70
PP-3/21		3,21	2,03	2,90	2,50	2,19	1,95	0,78
average		**3,23**	**2,54**	**2,77**	**2,27**	**1,88**	**1,61**	**0,70**
PP-3/22	7	5,01	4,14	4,23	3,39	2,59	2,09	0,68
PP-3/23		4,61	3,46	3,60	2,94	2,35	1,95	0,64
PP-3/24		5,16	3,92	4,31	3,29	2,47	1,98	0,64
average		**4,93**	**3,84**	**4,05**	**3,21**	**2,47**	**2,01**	**0,65**
PP-3/25	28	5,41	4,45	4,49	4,03	3,40	2,72	0,74
PP-3/26		5,78	4,40	4,62	3,95	3,06	2,40	0,68
PP-3/27		5,83	3,68	4,47	4,33	3,89	3,01	0,74
average		**5,67**	**4,18**	**4,53**	**4,10**	**3,45**	**2,71**	**0,72**
PP-3/28	56	5,78	4,03	4,62	3,71	2,67	2,06	0,64
PP-3/29		6,03	5,37	4,77	3,81	2,82	2,23	0,63
PP-3/30		5,92	4,85	4,74	3,93	2,85	2,25	0,66
average		**5,91**	**4,75**	**4,71**	**3,82**	**2,78**	**2,18**	**0,65**
PP-3/88	90	5,80	4,07	4,67	3,83	2,85	2,20	0,66
PP-3/89		5,33	4,42	4,56	3,73	2,74	2,14	0,70
PP-3/90		5,72	4,49	4,41	3,69	2,83	2,25	0,65
average		**5,62**	**4,33**	**4,55**	**3,75**	**2,81**	**2,20**	**0,67**

The ultimate splitting tensile strength f_{ct} increases uniformly with the age of PP-3 up to 56 days of age (third column in Table 7). After the first crack, the equivalent strengths decrease as the crack width increases (Figure 11). Softening occurs. The equivalent strengths at a given crack width increase from 3 to 28 days of age and then decrease so that the values at 56 and 90 days are of the same magnitude but less than those of 28-day-old PP-3.

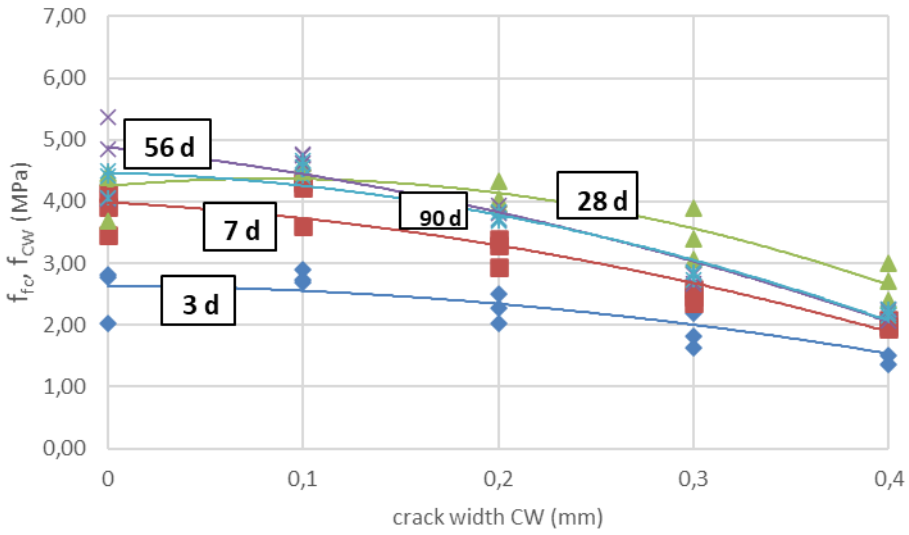

Figure 11. *Equivalent splitting tensile strengths f_{cw} and splitting tensile strength at first crack f_{fc} of PP-3 as a function of crack width.*

The resistance to crack propagation varies at different ages of PP-3; average RCP values from age 3 to 90 days are around 0,68 (last column in Table 7). All individual results are > 0,60.

In Figure 12, we give the results of the ultimate splitting tensile strength f_{ct} as a function of age for all HPC (PP-1, PP-1-JV, PP-2 and PP-3).

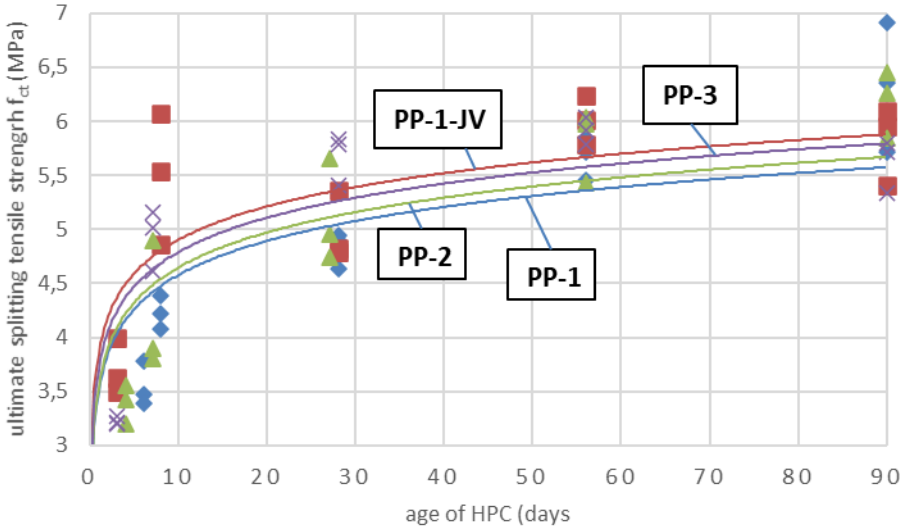

Figure 12*. Ultimate splitting tensile strength f_{ct} as a function of age for all HPC tested*

There are relatively small differences between the ultimate splitting tensile strengths f_{ct} at all HPC ages. There is also a significant dispersion of results.

However, there is a larger difference between the RCPs of PP-1-JV, which deviates in magnitude from the RCPs of the other three HPCs (Figure 13).

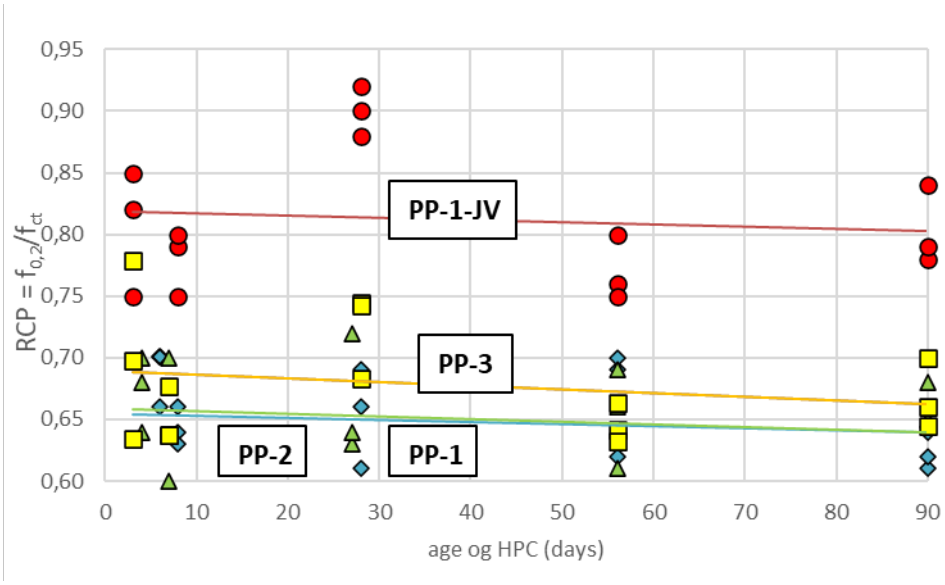

***Figure 13**. Resistance to crack propagation as a function of the age of HPC (PP-1, PP-1-JV, PP-2 and PP-3).*

This figure also shows that there is no correlation between RCP and HPC age; the RCP values of all HPCs do not change much on average with the age of the HPC, and there is a slight trend of decreasing average RCP values with the age of the HPC.

The RCP results of all HPCs meet the required criterion of RCP ≥ 0,60, which means that all HPCs show resistance to crack propagation. The RCP results obtained from PP-1-JV are relatively highest, around 0,80. All results for all ages PP-1-JV are greater than 0,75.

5. CONCLUSIONS

All the High-Performance Concretes (HPC) investigated in the project achieved very high durability in addition to high compressive strength due to their high-quality structure. However, to achieve a long service life of the structure, it is important that good resistance to crack propagation has been achieved in the HPC. The required RCP ≥ 0,60 was achieved at all HPC ages. The added steel fibers further improve the resistance of the HPC to crack propagation. The RCP = 0,75, which is often required in practice for Fiber Reinforced Concrete structures, was easily exceeded.

6. REFERENCES

[1] H.P. Reinhardt, "Hochleistungsbeton (High Performance Concrete)", *Betonwerk + Fertigteil-Technik*, Heft 1/1995 (Concrete Precasting Plant and Technology, Issue 1/1995). pp. 62 – 68, 1995

[2] O.E. Gjørv, "High-Strength Concrete. Advances in Concrete Technology", *CANMET*, pp. 21–77, 1992

[3] F. Young, "Very high strength cement-based materials", *Mat. Res. Soc.* Vol. 42, 1984. p. 317, 1984
[4] B. Hillemeier, "Innovationen am Baustoffmarkt - Neue Baustoffe sichern das Bauen", *Zement und Beton*, Wien. 1/96. pp. 1-8, 1996.
[5] P. Richard, M. Cheyrezy, "Composition of Reactive Powder Concretes", *Cement and Concrete Research*, Vol. 25, No. 7. pp. 1501 – 1511, 1995.
[6] M. Cheyrezy, V. Maret, L. Frouin, "Microstructural Analysis of RPC (Reactive Powder Concrete)", *Cement and Concrete Research*, Vol. 25, No. 7. pp. 1491 – 1500, 1995.
[7] S. P. Shah. „*High Strength Concrete*", University of Illinois at Chicago Circle, pp. 1-226, 1979.
[8] H. G. Russel, "High Strength Concrete", *ACI SP-87*. Detroit, pp. 1 - 278, 1985.
[9] Y. Malier, „ *Les bétons à hautes performances*", Presses de l'ENCP, Paris, pp. 1- 543, 1990.
[10] S. Kuroiwa, Y. Mutsuoka, M. Hayakawa, T. Shindoh, "Application of Super-workable Concrete to Construction of a 20-Story Building", *ACI SP-140*, pp. 147 – 161, 1993.
[11] P. Stroeven, "Struktura agregata v betonu in njen vpliv na cementno pasto", *Zbornik gradiv in referatov 13. slovenskega kolokvija o betonih: Agregati v betonu*. IRMA, Ljubljana, pp. 9 – 20, 2006.
[12] A. Zajc, „Uporaba mineralnih dodatkov v cementu in/ali betonu", IRMA. pp. 1-90, 2014.
[13] S. Mindess, J.F. Young, D. Darwin, „*Concrete",* Prentice Hall Inc Englewood Cliffs, pp.80-543, 2003.
[14] S. Diamond, S. Mindess, J. Lovell, "On the Spacing between Agreggate Grains in Concrete and the Dimension of the Aureaole of Transition", *RILEM Colloquium*, Toulouse, pp. C42 – C46, 1982.
[15] V. Rudert, J. Strunge, H.D. Wihler, „Beton aus anderer Sicht – filigranes Mikrogefüge", *Betonwerk + Fertigteil-Technik 60.* No. 9. pp. 86 – 93, 1994.
[16] J. Šušteršič, „Doseganje posebnih lastnosti betona z dodatki", *Zbornik gradiv in referatov 14. slovenskega kolokvija o betonih: Posebne lastnosti betonov z dodatki*, IRMA, Ljubljana, pp. 9 – 19. 2007
[17] E.K. Tschegg, „Prüfeinrichtung zur Ermittlung von bruchmechanischen Kenwerten sowie hiefür geeignete Prüfkörper", 1986.
[18] H. Linsbauer, E.K. Tschegg, „Die Bestimmung der Bruchenegie an Würfelproben". *Zement und Beton*. 31 (1986) 1, pp. 38 – 40, 1986.
[19] E.K. Tschegg, "Patent application No. 48/1990. Lasteinleitungsvorrichtung", 1990.
[20] E.K. Tschegg, "New Equipments for Fracture Tests on Concrete", *Materialprüfung* 33. 11 – 12. München, pp. 338 – 342, 1991.
[21] J. Šušteršič, R. Ercegovič, D. Polanec, A. Zajc,"Evaluation of behavior of the joint between two concrete layers during splitting", V: SERNA, Pedro (ed.). *Fibre reinforced concrete : improvements and innovations II : X RILEM-fib International Symposium on Fibre Reinforced Concrete (BEFIB) 2021*. Cham: Springer, cop. 2022. RILEM bookseries, vol. 36. pp. 208-219., 2022.
[22] L. Chen, S. Mindess,, D.R. Morgan, „Toughness Evaluation of Steel Fibre reinforced Concrete", *Proceedings of 3rd Canadian Symposium on Cement and Concrete*, Ottawa, pp. 16 – 29, 1993.
[23] D.R. Morgan, S. Mindess, L. Chen., „Testing and Specifying Toughness for Fibre Reinforced Concrete and Shotcrete", *Fibre Reinforced Concrete- Modern Developments.* Eds.: N. Banthia and S. Mindess. The University of British Columbia, Vancouver, pp. 29 – 50, 1995.
[24] J. Šušteršič, A. Zajc, I. Leskovar, V. Dobnikar, "Improvement in the crack opening resistance of FRC with low content of short fibres", Ed.: Dhir, Ravindra K. *Role of*

concrete in sustainable development: Proceedings of the International Symposium dedicated to professor Surendra Shah, Northwestern University, USA held on 3-4 September 2003 at the University of Dundee, Scotland, UK. London: ˝Thomas Telford. pp. 167-174, 2003.

[25] J. Šušteršič, R. Ercegovič, „Poročilo projekta Študija proizvodnje, vgradljivosti in karakteristik končnih betonskih mešanic za izvedbo sekundarne armiranobetonske obloge silosa odlagališča NSRAO“, IRMA, Ljubljana, pp. 1-646, 2020.

[26] B. Grujic, “Mikroarmirani beton – primjena u geotehnici”, Arhitektonsko-građevinsko-geodetski fakultet Univerzitet u Banjoj Luci, Banjaluka, 2022.

[27] O. Osamah, G. Emad, P. Tilak, L. Jessey, A. Kamiran, “Evaluation of Concrete Material PropertiesatEarly Age”, CivilEng 2022, 3(4), pp. 909-945, 2022.

AUTHOR'S BIOGRAPHIES

Jakob Šušteršič

Professor, employed at the IRMA Institute for Research in Materials and Applications, Slovenia

Rok Ercegovič

Civil engineer, employed at the IRMA Institute for Research in Materials and Applications, Slovenia.

David Polanec

Civil engineer with a Master's degree, employed at the IRMA Institute for Research in Materials and Applications, Slovenia.

Bojana Grujić

Professor at the Faculty of Architecture, Civil Engineering and Geodesy at the University of Banja Luka and Postdoctoral Researcher at Yamaguchi University in Japan.

ИСПИТИВАЊЕ ОТПОРНОСТИ БЕТОНА ВИСОКИХ ПЕРФОРМАНСИ НА ШИРЕЊЕ ПУКОТИНА МЕТОДОМ ЦИЈЕПАЊА КЛИНОМ

Сажетак: У овом раду се описују кључни елементи резултата истраживања отпорности на ширење пукотина спроведених у оквиру обимног пројекта развоја бетона високих перформанси (БВП) за секундарну облогу окна за одлагање радиоактивног отпада ниског и средњег нивоа. Истраживали смо четири састава БВП, у којима смо варирали количину везивне компоненте и међусобне односе два цемента и силикатне прашине. Такође смо додали челична влакна у један БВП. За одређивање отпорности на ширење пукотине кориштена је метода испитивања цијепања клином. Добијени резултати показују да сви испитивани БВП постижу добру отпорност на ширење пукптине. Додатак челичних влакана додатно побољшава ову отпорност.

Кључне ријечи: *отпорност на ширење пукотина, бетон високих перформанси, испитивање цепања клином*